American Journal of Advanced Research, 2019, 3–2
December. 2019, pages 20-25
doi: 10.5281/zenodo.3372446
http://ibii-us.org/Journals/AJAR/
ISBN 2572-8849 (Online), 2572-8830 (Print)

Aerodynamic Modeling of a Small-Scale Vertical Axis Wind Turbine

Jun Xu* and Adolfo Tovar

Department of Engineering and Computer Science, Tarleton State University, Stephenville, TX 76401.

*Email: junxu@tarleton.edu

Received on May 31, 2019; revised on 08/01/2019; published on 08/20/2019

Abstract

In this study, a small-scale five bladed 2D model was adopted to investigate the VAWT aerodynamics. A CFD model of the blades was created in ANSYS Fluent. The CFD results demonstrated that the model was capable of capturing the effect that the rotor encounters vortex interactions where the retreating blade impinges on its own wake and the wakes of other preceding blades. In addition, the results showed that as the rotational speed increases the downwind wake becomes more skewed, evidenced by the vorticity and turbulence kinetic energy fields. Based the simulation results, modeling limitations and recommendations were discussed regarding the current 2D modeling approach. Finally, future work and plan regarding 3D modeling were addressed.

Keywords: renewable energy, vertical axis wind turbine, CFD, aerodynamics

1 Introduction

With increasing interest in energy independence and sustainability, there is an urgent need to assess the reliability, efficiency, and performance of current and future power generation technologies. Wind energy is becoming more important due to its availability and relatively low impact on the surrounding environment. There are two types of wind turbines, Horizontal axis wind turbines (HAWT), and Vertical Axis Wind Turbines (VAWT). As the names would suggest, the HAWT rotates about a horizontal axis and the VAWT rotates about a vertical axis. HAWTs are generally used for more large scale electricity production, whereas VAWTs are more for small scale production. Modern wind farms with HAWTs have gradually increased in size over the years. Spacing between the turbines becomes an important issue for power losses due to wake interference from adjacent wind turbines in tightly spaced wind farms. On the other hand, wider spacing is considered expensive due to the high cost of land resources and installing power cables to the wind farm. Hence, there are substantial benefits to be gained from using smaller wind turbines to minimize operational and maintenance costs.

While VAWTs may not be the largest electricity generators, they have some key advantages such as low cost, simple setup, easy maintenance. All of these advantages lend VAWT to be used for small scale electricity production in areas where limited space is a factor and areas where there is high wind speed. Examples include the tops of buildings, where the building will redirect wind to the turbine increasing power production, remote mountain ranges, and urban environments.

CFD study of VAWT has been the focus of several recent investigations (Elkhour, Kiwata, Nagao, Kono, & ElHajj, 2018; Franchina, Persico, & Savini, 2019; Hand & Cashman, 2018; Hezaveh et al., 2018; Hui, Cain, & Dabiri, 2018; Rezaeiha, Kalkman, Montazeri, & Blocken, 2017; Rezaeiha, Montazeri, & Blocken, 2018a, 2018b; Rogowski, 2018; Rogowski, Maronski, & Piechna, 2017; Shah, Kumar, Raahemifar, & Fung, 2018). For instance, a two-step approach was adopted to investigate 2D and 3D VAWT aerodynamics and it was found that 3D effects must be included to provide an accurate prediction of VAWT performance especially at high tip speed ratios (3). A detailed comparison study was carried out to examine a small scale VAWT using 2D and 3D CFD (2). Despite the advantage of full 3D CFD simulation, such simulations require a very large computational cost which makes these models still prohibitive for design purposes.

To reduce the computational cost, in this study we employed a simplified 2D Computational Fluid Dynamics (CFD) approach to address the question of how the rotational speed affects aerodynamic characteristics of a small-scale VAWT. The 2D approach was justified since our tip speed ratios were quite low.

2 Methods

The wind turbine we modeled is the same model that was used in a recent physical experiment conducted at Princeton University to investigate dynamic similarity (Miller et al., 2018). Further details can be found in that paper. The small five-bladed model turbine was based on a commercial design by Wing Power Energy with a 1/22.5 scale ratio.

2.1 Geometry and mesh

Figure 1 shows the final, fully assembled 3D VAWT used in this study. Table 1 shows the main dimensions of the turbine (Miller et al., 2018). The location of the cutting plane to create the 2D cross-section is indicated by the black cutting line.

Table 1. Turbine main dimensions

Number of blade	5
Diameter, mm	96.6
Span, mm	162.58
Cord length, mm	21.63
Turbine hub diameter, mm	25.4

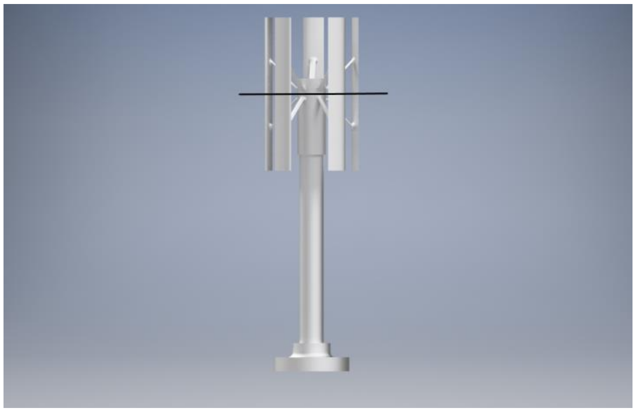

Figure 1: 3d solid model of a five-bladed VAWT

Figure 2 shows the detailed view of the rotor. Each blade has a profile that is the same as NACA 0021 airfoil. This airfoil has been very popular in VAWT designs. Each blade was held in place by two slender structural members.

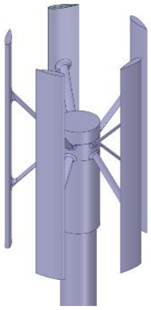

Figure 2: 3d blade model

The simulation was done in 2D with the cross-sectional view of the airfoils and main shaft of the VAWT studied as shown in Figure 3.

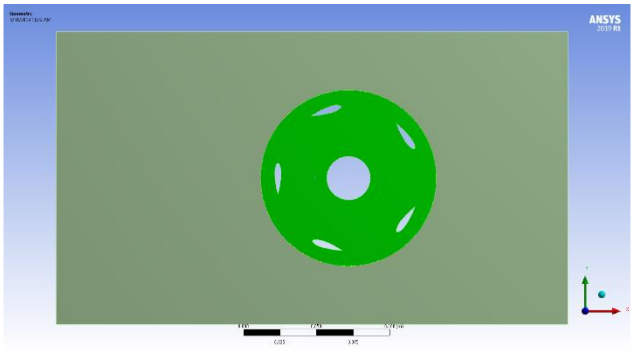

Figure 3: 2d model of a cross-sectional cut of the full model that was made at the middle of the blade and pillar assembly

Figure 4 shows the mesh used in the simulations and Figure 5 shows the mesh details around the each blade and hub.

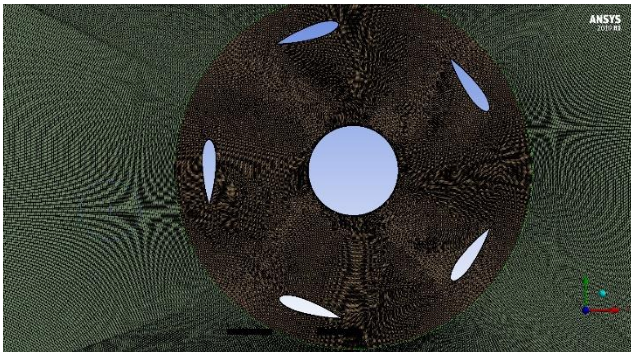

Figure 4: Full computational mesh used in simulation

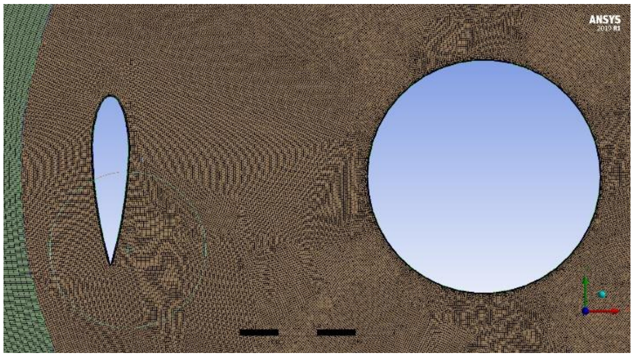

Figure 5: Details of mesh around each blade and the bub

2.2 Computational model

The transient turbulent flow field around the small-scale turbine is often treated as incompressible due to the low Ma number. The governing equations are Navier-Stokes equation. The chosen governing equations used to compute the turbulent flow is k-ε viscous model. This is a common equation used to model turbulent flow in CFD.

To capture the complex flow field of the model turbine, all computations were done in ANSYS Fluent 2019. Sliding mesh approach was used to deal with the relative motion between the rotating turbine and the flow domain. In this study we assumed that the turbine was already spinning independently of the flow. Please note that this is an over-simplification of the physical reality, since the flow is impinging on the blades for spinning the turbine in the first place. To couple the rotation with the incoming flow to start the rotation from a static condition is a challenging problem. Currently, efforts are still underway in this active research area (Balduzzi et al., 2017; Untaroiu, Wood, Allaire, & Ribando, 2011). Based on the mass moment inertia of the turbine, the rotating rate can be determined by the incoming flow velocity. However, modeling the movement of a solid body caused by the flow is considerably difficult, and requires the use of a two-way fluid-structure interaction.

2.3 Initial and boundary conditions

Figure 6 shows the computational domain. The computational domain consists of two parts, an inner one, which defines the moving frame region (the circle with the shat and airfoil sections), and an outer one, which defines the steady far field region. Initially, the x direction velocity U was set to 10 m/s. Inlet velocity was set to 10 m/s, and outlet gage pressure was set to 0 Pa. Symmetry condition was set for either side as shown in Figure 6. The turbine was set to spin at 40 and 80 rpm, respectively. The inlet turbulent intensity was set to 0.3% and turbulent length scale was set to 0.0015 m. The time step was set to 0.05 sec for a total 5 sec of running time.

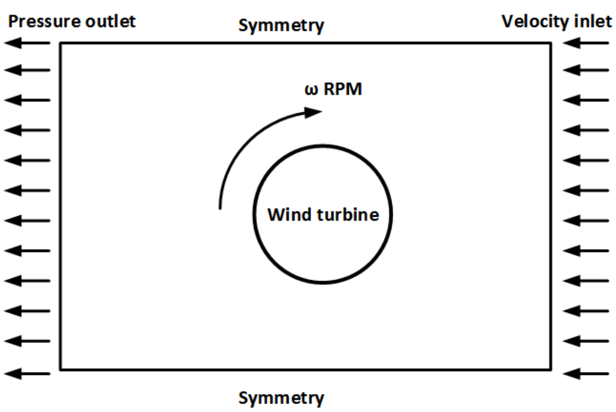

Figure 6: Schematic of computational domain

3 Results and discussion

Two conditions were conducted. One where the rotational velocity of the VAWT was set at 40 rpm and the other one where it was 80 rpm. The corresponding TSRs were 0.02 and 0.04, respectively. The tip speed ratio (TSR) was calculated as

$$TSR = \omega R / V \quad (1)$$

where V is the inlet velocity and ω is the rotational speed.

Figure 7 shows the vorticity contours at 1.0, 1.1, and 1.2 sec with the rotor rotating at 40 rpm clockwisely (TSR=0.02). It is clear that the 2D CFD model is able to produce the rotating effects quite nicely and flow field is clearly biased due to the rotation. Furthermore, the CFD results demonstrate that the model is capable of capturing the cascading effect of the rotor's wake where the retreating blade impinges on its own wake and the wakes of other preceding blades as indicated in Figure 7A-7C.

(A)

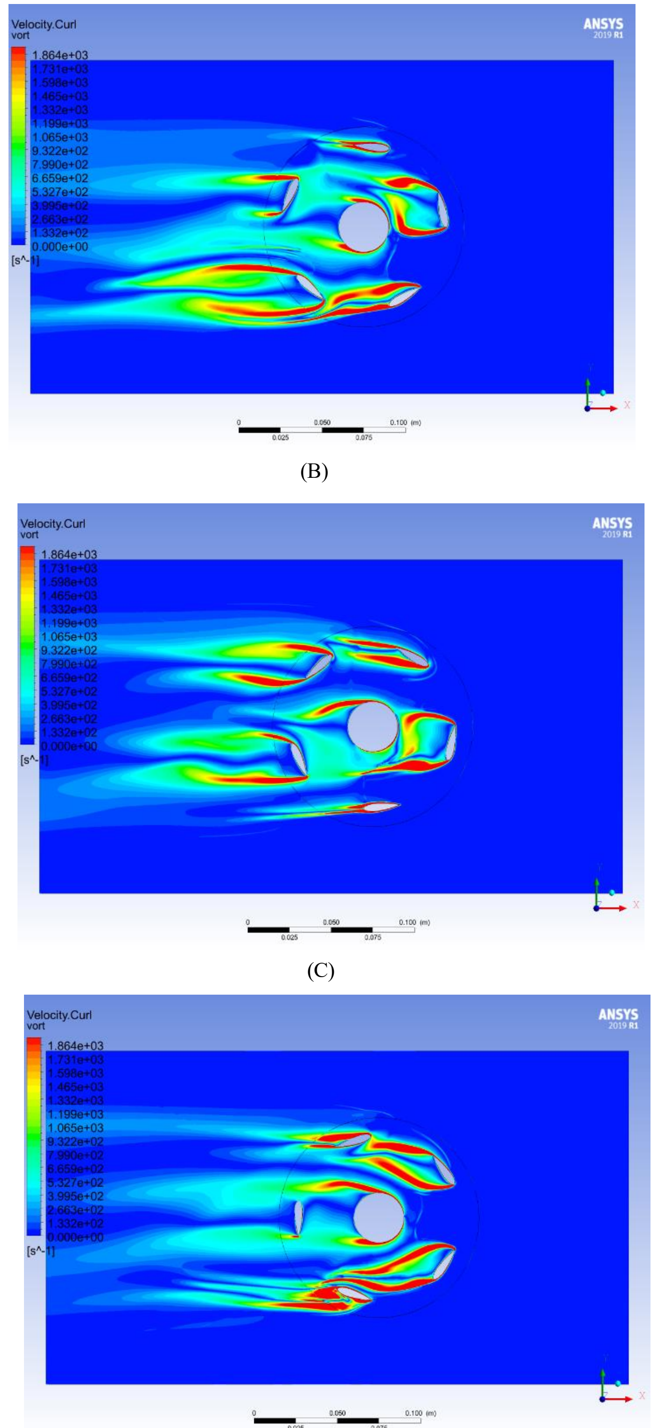

Figure 7: Vorticity at (A) 1.0, (B) 1.1, AND (C) 1.2 sec for 40 rpm

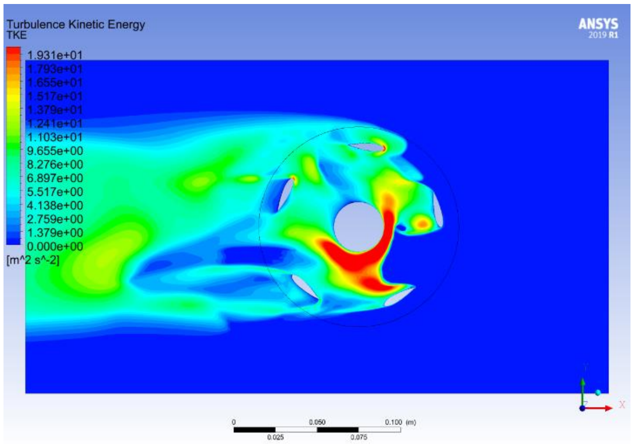

(A)

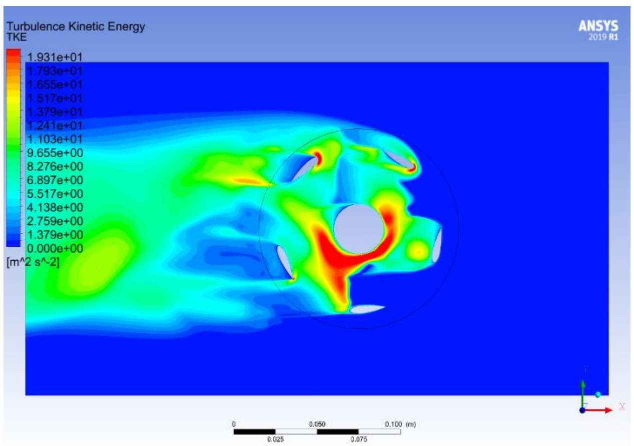

(B)

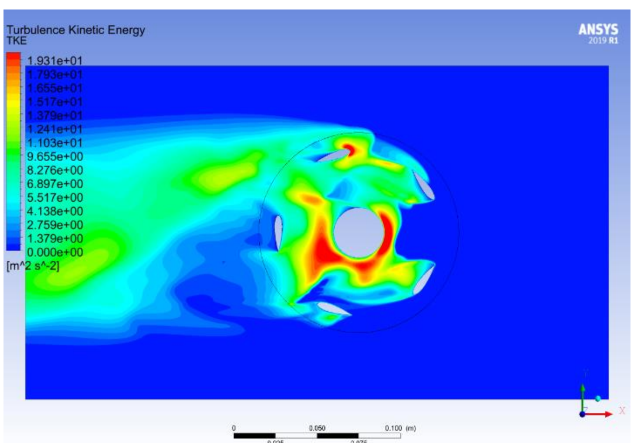

(C)

Figure 8: Turbulent kinetic energy at (A) 1.0, (B) 1.1, AND (C) 1.2 sec (40 rpm)

Figure 8 shows the turbulence kinetic energy distribution around the blades and the hub at 40 rpm, clearly indicating the high turbulence around the hub.

Figure 9 shows the pressure (left) and velocity contours (right) at 1.0 sec with 40 rpm rotor speed (TSR=0.02).

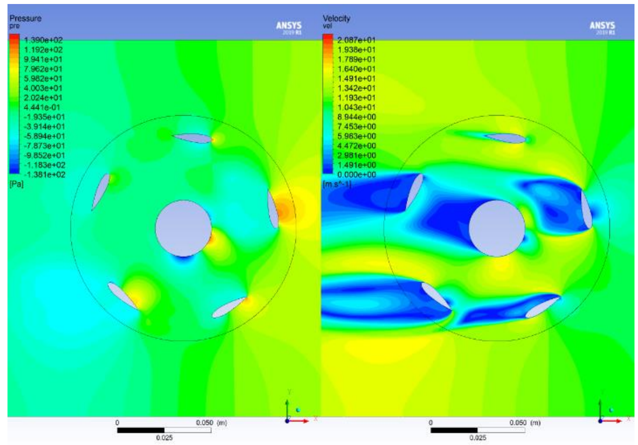

Figure 9: Pressure (left) and velocity (right) at 1.0 sec (40 rpm)

Figure 10 shows the vorticity at 1, 1.1, and 1.2 sec with rotor moving at 80 rpm (TSR=0.04). Similar to the case at 40 rpm, the rotational effects are nicely reproduced. Blades at different spatial locations have drastically different flow fields. It is interesting to note that the interaction of the wake of the right-most blade with the rotor hub (Figure 10A), clearly indicating the importance of including the hub in the simulation. In contrast to Figure 7, however, the flow fields are evidently more skewed at 80 rpm than those at 40 rpm, indicating the increasing disturbance at higher rotation rates.

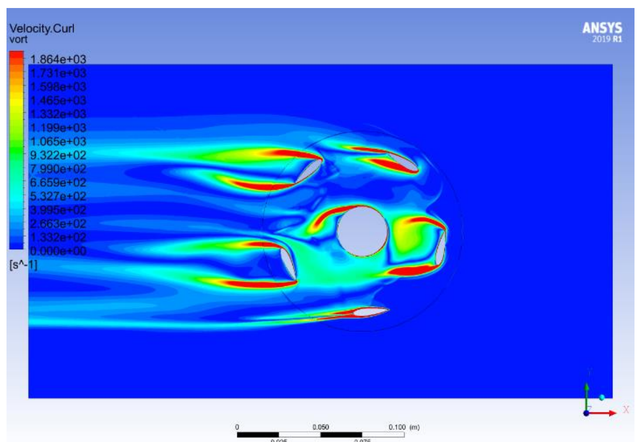

(A)

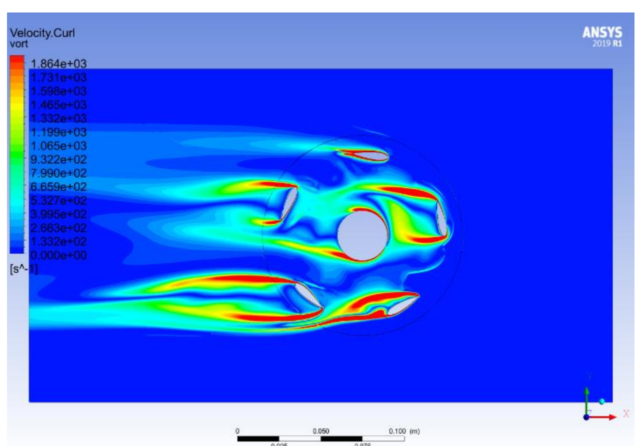

(B)

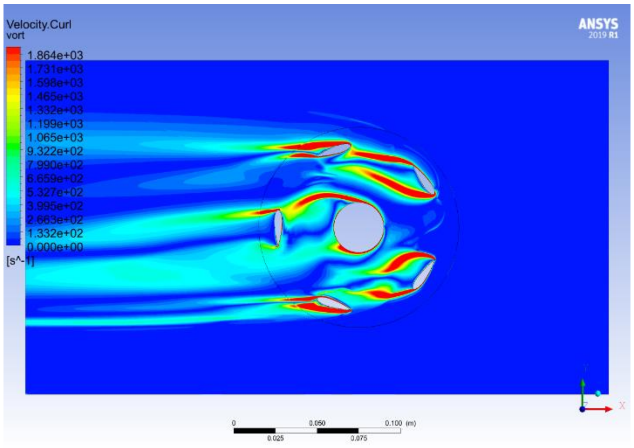

(C)

Figure 10: Vorticity at (a) 1.0, (b) 1.1, and (c) 1.2 sec at 80 rpm

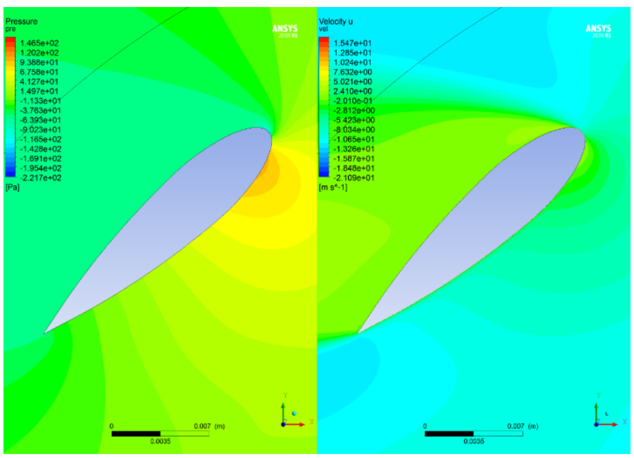

Figure 11: Pressure (left) and x-direction velocity (right) around a blade at 80 rpm.

Figure 11 shows the close-up view of pressure (left) and U velocity (right) comparison at 80 rpm rotation rate. The high pressure (red tinted area) in the pressure contour corresponds with the low positive velocity (the green area) in the velocity counter at the leading edge. This is a visual representation of the lift caused by the air flowing over the airfoil.

4 Conclusion

In present work, an unsteady-state 2D model of VAWT was constructed to investigate aerodynamic characteristics of a small scale rotor. To capture the unsteady state rotational effects, a sliding mesh approach was employed. Despite the limitations faced using 2D geometry, the CFD results demonstrated that the 2D model was capable of capturing the essential features of the flow field around the rotor given the low tip speed ratios in our study. Our future work will include investigating lift and power coefficients and compare with experimental data. We also plan to implement 3D simulations, which could provide increased accuracy and capture 3D effects such as tip vortex more precisely at higher TSRs.

Acknowledgements

The author wishes to gratefully acknowledge the financial support provided by the Tarleton State University Office of Research and Innovations. The author would also like to thank Dr. Mark A. Miller for providing solid model data.

Funding

This work has been supported by the Tarleton State University Faculty-Student Research and Creative Activity Internal Grant.

Conflict of Interest: none declared.

References

Balduzzi, F., Drofelnik, J., Bianchini, A., Ferrara, G., Ferrari, L., & Campobasso, M. S. (2017). Darrieus wind turbine blade unsteady aerodynamics: a three-dimensional Navier-Stokes CFD assessment. *Energy*, *128*, 550-563. doi:10.1016/j.energy.2017.04.017

Elkhour, M., Kiwata, T., Nagao, K., Kono, T., & ElHajj, F. (2018). Wind tunnel experiments and Delayed Detached Eddy Simulation of a three-bladed micro vertical axis wind turbine. *Renewable Energy*, *129*, 63-74. doi:10.1016/j.renene.2018.05.096

Franchina, N., Persico, G., & Savini, M. (2019). 2D-3D Computations of a Vertical Axis Wind Turbine Flow Field: Modeling Issues and Physical Interpretations. *Renewable Energy*, *136*, 1170-1189. doi:10.1016/j.renene.2018.09.086

Hand, B., & Cashman, A. (2018). Aerodynamic modeling methods for a large-scale vertical axis wind turbine: A comparative study. *Renewable Energy*, *129*, 12-31. doi:10.1016/j.renene.2018.05.078

Hezaveh, S. H., Bou-Zeid, E., Dabiri, J., Kinzel, M., Cortina, G., & Martinelli, L. (2018). Increasing the Power Production of Vertical-Axis Wind-Turbine Farms Using Synergistic Clustering. *Boundary-Layer Meteorology*, *169*(2), 275-296. doi:10.1007/s10546-018-0368-0

Hui, I., Cain, B. E., & Dabiri, J. O. (2018). Public receptiveness of vertical axis wind turbines. *Energy Policy*, *112*, 258-271. doi:10.1016/j.enpol.2017.10.028

Miller, M. A., Duvvuri, S., Brownstein, I., Lee, M., Dabiri, J. O., & Hultmark, M. (2018). Vertical-axis wind turbine experiments at full dynamic similarity. *Journal of Fluid Mechanics*, *844*, 707-720. doi:10.1017/jfm.2018.197

Rezaeiha, A., Kalkman, I., Montazeri, H., & Blocken, B. (2017). Effect of the shaft on the aerodynamic performance of urban vertical axis wind turbines. *Energy Conversion and Management*, *149*, 616-630. doi:10.1016/j.enconman.2017.07.055

Rezaeiha, A., Montazeri, H., & Blocken, B. (2018a). Characterization of aerodynamic performance of vertical axis wind turbines: Impact of operational parameters. *Energy Conversion and Management*, *169*, 45-77. doi:10.1016/j.enconman.2018.05.042

Rezaeiha, A., Montazeri, H., & Blocken, B. (2018b). Towards optimal aerodynamic design of vertical axis wind turbines: Impact of solidity and number of blades. *Energy*, *165*, 1129-1148. doi:10.1016/j.energy.2018.09.192

Rogowski, K. (2018). Numerical studies on two turbulence models and a laminar model for aerodynamics of a vertical-axis wind turbine. *Journal of Mechanical Science and Technology*, *32*(5), 2079-2088. doi:10.1007/s12206-018-0417-0

Rogowski, K., Maronski, R., & Piechna, J. (2017). Numerical Analysis of a Small-Size Vertical-Axis Wind Turbine Performance and Averaged Flow Parameters around the Rotor. *Archive of Mechanical Engineering, 64*(2), 205-218. doi:10.1515/meceng-2017-0013

Shah, S. R., Kumar, R., Raahemifar, K., & Fung, A. S. (2018). Design, modeling and economic performance of a vertical axis wind turbine. *Energy Reports, 4*, 619-623. doi:10.1016/j.egyr.2018.09.007

Untaroiu, A., Wood, H. G., Allaire, P. E., & Ribando, R. J. (2011). Investigation of Self-Starting Capability of Vertical Axis Wind Turbines Using a Computational Fluid Dynamics Approach. *Journal of Solar Energy Engineering-Transactions of the Asme, 133*(4). doi:Artn 041010/10.1115/1.4004705